I N F O R M A T I K

A Framework for Evaluating the Quality of Lossy Image Compression

Jörg Haber   Hans-Peter Seidel

MPI–I–1999–4-001   December 1999

FORSCHUNGSBERICHT   RESEARCH REPORT

M A X - P L A N C K - I N S T I T U T
F Ü R
I N F O R M A T I K

Im Stadtwald   66123 Saarbrücken   Germany

Author's Address

Jörg Haber, Hans-Peter Seidel
Computer Graphics Group
Max-Planck-Institut für Informatik
Im Stadtwald, 66123 Saarbrücken, Germany
Email: {haberj, hpseidel}@mpi-sb.mpg.de

Abstract

In this research report we present a framework for evaluating and comparing the quality of various lossy image compression techniques based on a multiresolution decomposition of the image data. In contrast to many other publications, much attention is paid to the interdependencies of the individual steps of such compression techniques. In our result section we are able to show that it is quite worthwile to fine-tune the parameters of every step to obtain an optimal interplay among them, which in turn leads to a higher reconstruction quality.

Keywords

image compression – wavelet transform – quantization – quality evaluation

1 Introduction

State-of-the-art algorithms for lossy still image compression are usually based on a multiresolution decomposition of the image data. The idea behind this technique has already been introduced in [BA83], the complete compression scheme was described in [ABDM92]. Due to a fast algorithm for a discrete wavelet transform published in [Mal89], this technique allows for high quality image compression in a fraction of the time needed for instance by fractal compression techniques such as [Jac92] or [Sau95].

The principle of such wavelet-based lossy image compression techniques can be grouped into three generic steps:

compression

1. basis transform of the image data;
2. quantization of the transformed coefficients;
3. coding of the quantized coefficients.

Each of these steps will be described in more detail in the following sections 2–4. Since usually steps 1 and 3 are losslessly invertible, the lossy compression happens in step 2.

The decompression is done in a straightforward way, which can be described again in three steps:

decompression

1. decoding of the compressed data;
2. dequantization of the decoded coefficients;
3. inverse basis transform of the dequantized coefficients.

Obviously, the second step will introduce some approximation error, since the quantization step in the compression scheme is not losslessly invertible. Thus, the approximated dequantized coefficients fed into the inverse basis transform step in the decompression scheme will be transformed into an approximation of the original image data. It is up to the design and implementation of every step and the interplay of all these steps to produce an approximation error as small as possible given a fixed compression ratio.

Even though a lot of work has been published on the examination of each step, cf. for example [OB96, HSW95, CS94, VBL95, CW90, Wic90, CW92] on step 1,

[Llo82, LBG80, Equ89, ABM91] on step 2 and [GG92, Sha93, VTC96] on step 3, there are only few publications to our knowledge that take into account at least some of the very important interdependecies of these three steps, cf. [Bal98].
Unfortunately, not all of these interdependencies can be motivated mathematically. In this case, an optimal set of parameters for each step has to be found heuristically. Evaluating all reasonable combinations of parameters can become a very time-consuming task. However, our results show that for a whole scenario of images, a set of sub-optimal parameters can be given, which produces an approximation error close to the optimal one in the average. The term *scenario of images* in our terminology denotes a collection of images, which are similar to each other by some means.

2 Transformation

The first step in the compression scheme is given by a basis transform of the image data. The objective of this transform is to reduce the entropy of the input data. Due to [Kar47, Loè48], the Karhunen-Loève transform is optimal in this sense. Unfortunately, the computational overhead for this transform is too big for practical applications. On the other hand, a (discrete) wavelet transform has proven to be a good compromise between computational time and entropy reduction. Particularly for use in lossy image compression, another transform has gained wide-spread popularity: the discrete cosine transform (DCT), as it is used e.g. in the JPEG standard [PM93]. However, because of the local support of the associated filter, a block structure artifact becomes clearly visible in the reconstructed images, especially when using high compression ratios. This makes the DCT rather unalluring for high quality image compression.

2.1 Wavelet Theory

In this section we will give a brief overview of wavelet theory as far as it applies to image compression. Good introductory textbooks on wavelet theory have been written by many authors, see for instance [Chu92, Dau92, Mey92, VK95, SN96]. Among the many approaches to wavelet theory the introduction of a multiresolution analysis (MRA) by MALLAT [Mal89] seems to be most appropriate for image compression. An MRA of the $L^2(\mathbb{R})$ is a nested sequence of closed subspaces $V_j \subset L^2(\mathbb{R})$:

$$\{0\} \subset \ldots \subset V_{-1} \subset V_0 \subset V_1 \subset \ldots \subset L^2(\mathbb{R}) \tag{1}$$

such that

$$\overline{\bigcup_{j\in\mathbb{Z}} V_j} \;=\; L^2(\mathbb{R}) \tag{2}$$

$$\bigcap_{j\in\mathbb{Z}} V_j \;=\; \{0\} \tag{3}$$

$$f(\cdot)\in V_j \iff f(2^{-j}\,\cdot)\in V_0 \tag{4}$$

$$\exists\,\varphi\in L^2(\mathbb{R}) \qquad \text{with} \qquad V_0 \;=\; \overline{\operatorname{span}\{\varphi(\cdot-k)\mid k\in\mathbb{Z}\}}\;. \tag{5}$$

If in addition $\{\varphi(\cdot-k)\mid k\in\mathbb{Z}\}$ is a Riesz basis of V_0 with some Riesz bounds $0<A\le B<\infty$, then it follows that for each $j\in\mathbb{Z}$ the family $\{\varphi_{j,k}\mid k\in\mathbb{Z}\}$ is a Riesz basis of V_j, where

$$\varphi_{j,k}(x) \;:=\; 2^{j/2}\,\varphi(2^jx-k)\;. \tag{6}$$

Such a function $\varphi\in L^2(\mathbb{R})$ is called a *scaling function*, if the subspaces

$$V_j := \overline{\operatorname{span}\{\varphi_{j,k}\mid k\in\mathbb{Z}\}}\in L^2(\mathbb{R}) \quad (j\in\mathbb{Z})$$

satisfy the properties (1), (2) and (4).
A scaling function φ is said to generate an MRA. It can be shown that there exists a unique sequence $\{h_k\}$ $(h_k\in\mathbb{R}, k\in\mathbb{Z})$ so that the so-called *two-scale relation* holds:

$$\varphi(x) \;=\; \sqrt{2}\sum_k h_k\,\varphi(2x-k)\;. \tag{7}$$

With the help of our function φ we can now define the associated (mother) wavelet

$$\psi(x) \;:=\; \sqrt{2}\sum_k g_k\,\varphi(2x-k) \tag{8}$$

with

$$g_k := (-1)^k\,h_{1-k}\;\in\mathbb{R}\;, \tag{9}$$

and, analogously to (6), its dilated and translated versions

$$\psi_{j,k}(x) \;:=\; 2^{j/2}\,\psi(2^jx-k)\;. \tag{10}$$

Since $\{\psi_{j,k}\mid k\in\mathbb{Z}\}$ is now an orthonormal basis of W_j, where

$$V_j\oplus W_j = V_{j+1} \quad (j\in\mathbb{Z})\;,$$

it follows that

$$L^2(\mathbb{R}) \;=\; \bigoplus_j W_j \;, \tag{11}$$

i.e. $\{\psi_{j,k} \mid j,k \in \mathbb{Z}\}$ is an orthonormal basis of the $L^2(\mathbb{R})$. Thus any function $f \in L^2(\mathbb{R})$ can be represented as a linear combination of the basis functions $\psi_{j,k}$:

$$f(x) \;=\; \sum_{j,k} d_{j,k}\, \psi_{j,k}(x) \;. \tag{12}$$

2.2 Discrete Wavelet Transform

A multiresolution analysis of the $L^2(\mathbb{R})$ as it was introduced by MALLAT [Mal89] does not only lead to the construction of a wavelet ψ, but in addition delivers an algorithm for a fast, discrete wavelet transform (DWT).
Let $f \in V_0 \subset L^2(\mathbb{R})$. According to (5), f can be written as

$$f(x) \;=\; \sum_k c_k^0\, \varphi(x-k)$$

with real coefficients

$$c_k^0 \;:=\; \langle f, \varphi_{0,k}\rangle_{L^2(\mathbb{R})} \;.$$

By using the notation

$$\begin{aligned} c_k^m &:= \langle f, \varphi_{m,k}\rangle_{L^2(\mathbb{R})} \;, \\ d_k^m &:= \langle f, \psi_{m,k}\rangle_{L^2(\mathbb{R})} \;, \end{aligned}$$

one yields with the help of the two-scale relation (7) the recursive identities:

$$\begin{aligned} c_k^m &= \sum_l h_l\, \langle f, \varphi_{m+1,2k+l}\rangle_{L^2(\mathbb{R})} = \sum_l h_l\, c_{2k+l}^{m+1} \;=\; \sum_l h_{l-2k}\, c_l^{m+1} \;, \\ d_k^m &= \sum_l g_l\, \langle f, \varphi_{m+1,2k+l}\rangle_{L^2(\mathbb{R})} \;=\; \sum_l g_l\, c_{2k+l}^{m+1} \;=\; \sum_l g_{l-2k}\, c_l^{m+1} \;. \end{aligned}$$

These recursive formulas can be rewritten as

$$\begin{aligned} c^m &= Hc^{m+1} \;, \\ d^m &= Gc^{m+1} \;, \end{aligned} \tag{13}$$

$$
\begin{tikzcd}
c^0 \arrow[r, "H"] \arrow[dr, "G"'] & c^{-1} \arrow[r, "H"] \arrow[dr, "G"'] & c^{-2} \arrow[r, "H"] \arrow[dr, "G"'] & \cdots \arrow[r, "H"] \arrow[dr, "G"'] & c^{-M+1} \arrow[r, "H"] \arrow[dr, "G"'] & c^{-M} \\
& d^{-1} & d^{-2} & \cdots & d^{-M+1} & d^{-M}
\end{tikzcd}
$$

Figure 1: Wavelet decomposition of the signal c^0 with M levels of resolution

$$
\begin{tikzcd}
c^{-M} \arrow[r, "H^*"] & c^{-M+1} \arrow[r, "H^*"] & c^{-M+2} \arrow[r, "H^*"] & \cdots \arrow[r, "H^*"] & c^{-1} \arrow[r, "H^*"] & c^0 \\
d^{-M} \arrow[ur, "G^*"'] & d^{-M+1} \arrow[ur, "G^*"'] & d^{-M+2} \arrow[ur, "G^*"'] & \cdots \arrow[ur, "G^*"'] & d^{-1} \arrow[ur, "G^*"'] &
\end{tikzcd}
$$

Figure 2: Reconstruction of the signal c^0 from M levels of resolution

with $c^m := \{c_k^m\}_{k\in\mathbb{Z}}$, $d^m := \{d_k^m\}_{k\in\mathbb{Z}}$ and

$$
\begin{aligned}
H:\ \ell^2(\mathbb{Z}) \ &\rightarrow\ \ell^2(\mathbb{Z}) \\
c\ &\mapsto\ Hc\ =\ \left\{\sum_l h_{l-2k}\, c_l\right\}_{k\,\in\,\mathbb{Z}},
\end{aligned}
\tag{14}
$$

$$
\begin{aligned}
G:\ \ell^2(\mathbb{Z}) \ &\rightarrow\ \ell^2(\mathbb{Z}) \\
c\ &\mapsto\ Gc\ =\ \left\{\sum_l g_{l-2k}\, c_l\right\}_{k\,\in\,\mathbb{Z}}.
\end{aligned}
\tag{15}
$$

The process of decomposing a signal c^0 into M levels of resolution is depicted in Figure 1. The inversion of this decomposition is called the reconstruction of c^0 (see Figure 2). It is given by

$$
c^{m+1}\ =\ H^*c^m\ +\ G^*d^m \tag{16}
$$

with

$$
\begin{aligned}
H^*c\ &=\ \left\{\sum_l h_{k-2l}\, c_l\right\}_{k\,\in\,\mathbb{Z}}, \\
G^*c\ &=\ \left\{\sum_l g_{k-2l}\, c_l\right\}_{k\,\in\,\mathbb{Z}}.
\end{aligned}
$$

2.3 Two-Dimensional Wavelet Transform

A straightforward construction of a two-dimensional wavelet transform was proposed MALLAT [Mal89]. In the context of image compression, however, a tensor product wavelet transform is commonly used. If we define (analogously to Eqs. (14),(15)) new decomposition operators H_l, G_l and H_c, G_c that operate on the lines and on the columns of an image f, respectively, the two-dimensional wavelet transform of f yields the following four sub-images:

$$
\begin{aligned}
f_{LL} &= H_c\, H_l\, f \ , \\
f_{LH} &= G_c\, H_l\, f \ , \\
f_{HL} &= H_c\, G_l\, f \ , \\
f_{HH} &= G_c\, G_l\, f \ .
\end{aligned}
\tag{17}
$$

The reconstruction of the image f is obtained by applying the corresponding adjuct operators $H_l^*, G_l^*, H_c^*, G_c^*$ to these sub-images:

$$
\begin{aligned}
f &= H_l^*\, H_c^*\, f_{LL} \;+\; H_l^*\, G_S^*\, f_{LH} \;+\; G_l^*\, H_c^*\, f_{HL} \;+\; G_l^*\, G_S^*\, f_{HH} \\
&= H_l^*\, [H_c^*\, f_{LL} \;+\; G_c^*\, f_{LH}] \;+\; G_l^*\, [H_c^*\, f_{HL} \;+\; G_c^*\, f_{HH}] \ .
\end{aligned}
\tag{18}
$$

MALLAT Algorithm

The MALLAT algorithm [Mal89] for a two-dimensional discrete wavelet transform with M levels of resolution is obtained by iterating the decomposition scheme (Eq. (17)) in the same way as it was shown for one-dimensional signals in Section 2.2. Using the notation from Section 2.3, the MALLAT algorithm with M levels of resolution can be written as:

$$
\begin{aligned}
f^{(0)} &\rightarrow \left\{ f_{LL}^{(1)}, f_{LH}^{(1)}, f_{HL}^{(1)}, f_{HH}^{(1)} \right\} \\
&\rightarrow \left\{ f_{LL}^{(2)}, f_{LH}^{(2)}, f_{HL}^{(2)}, f_{HH}^{(2)}, f_{LH}^{(1)}, f_{HL}^{(1)}, f_{HH}^{(1)} \right\} \\
&\ \ \vdots \\
&\rightarrow \Big\{ f_{LL}^{(M)}, f_{LH}^{(M)}, f_{HL}^{(M)}, f_{HH}^{(M)}, \\
&\qquad f_{LH}^{(M-1)}, f_{HL}^{(M-1)}, f_{HH}^{(M-1)}, \\
&\qquad\qquad \vdots \\
&\qquad f_{LH}^{(1)}, f_{HL}^{(1)}, f_{HH}^{(1)} \Big\} \ .
\end{aligned}
$$

In this scheme, the upper index in parantheses denotes the level of resolution. The set of sub-images obtained by the MALLAT algorithm for $M = 3$ is shown in Figure 3(b).

(a) original image (b) MALLAT algorithm (c) best-basis algorithm

Figure 3: Comparison of MALLAT Algorithm and Best-Basis Algorithm

Best-Basis Algorithm

In contrast to the MALLAT algorithm, the best-basis algorithm introduced by COIFMAN and WICKERHAUSER [CW92] performs a decomposition of every sub-image from the previous level of resolution to obtain the sub-images of the next level. From the (redundant) set of sub-images obtained by this decomposition process a subset is chosen subsequently. This subset is chosen to be both sufficient for lossless reconstruction of the original image and optimal in a certain sense.
A common optimality condition is to minimize the sum of the pseudo-entropies of all sub-images. The *pseudo-entropy* of a sub-image $s = (s_{i,j})_{i,j}$ is defined by:

$$E(s) \;:=\; -\sum_{i,j} s_{i,j}^2 \, \log_2 s_{i,j}^2 \tag{19}$$

with the predefinition $0 \cdot \log_2 0 := 0$.
Starting with the sub-images $f_{j,(i)}^{(M)}$ ($j \in \{LL,\ LH,\ HL,\ HH\} := \{0,1,2,3\}$, $i = 1,\ldots,4^{M-1}$) of the finest level $m := M$, the sum of the pseudo-entropies of each quadrupel $f_{j,(i)}^{(m)}$, ($j = 0,\ldots,3$) is compared to the pseudo-entropy of the corresponding sub-image $f_{j,(k)}^{(m-1)}$ ($j = i \bmod 4, k = \lfloor \frac{i}{4} \rfloor$) of the coarser level $m-1$. If

$$\sum_{j=0}^{3} E(f_{j,(i)}^{(m)}) \;<\; E(f_{i \bmod 4,(\lfloor \frac{i}{4} \rfloor)}^{(m-1)}) \;,$$

the four sub-images $f_{j,(i)}^{(m)}$, ($j = 0,\ldots,3$) are kept and the sum of their pseudo-entropies is assigned to the sub-image $f_{i \bmod 4,(\lfloor \frac{i}{4} \rfloor)}^{(m-1)}$, otherwise the four sub-images of level m are discarded. This process is carried out for all levels $m = M,\ldots,1$.

In the end, a subset of sub-images remains, that fulfils both the reconstruction and the optimality condition. A possible set of sub-images generated by the best-basis algorithm for $M = 3$ is shown in Figure 3(c).

3 Quantization

After a wavelet transform has been applied to the image data, the resulting real wavelet coefficients are mapped to some integer symbols. It is obvious, that in general this step cannot be reverted without introducing some approximation error. Thus the design of the quantization step plays an important role for the reconstruction quality. A *scalar quantization* quantizes every single wavelet coefficient seperately, a *vector quantization* groups several wavelet coefficients together and maps this coefficent vector to a single output symbol. The latter is usually more efficient, but also computationally more expensive.

3.1 Scalar Quantization

A uniform scalar quantization can be obtained by equidistant partitioning of the interval of the real coefficients into n subintervals. These subintervals (*quantization intervals*) are numbered from $0, \ldots, n-1$, and for every wavelet coefficient the number of its subinterval is output to the coder. Because of the following coding step, n should generally be chosen to be a power of 2. During the dequantization step, the midpoint of every quantization interval is used as an approximation for all the coefficients in this interval. This choice is known to minimize the average approximation error in an L^2 norm, cf. [Say96, GG92].
Since wavelet coefficients[1] have an expected value of $\mu = 0$, it is advantageous to use an odd number (e.g. $n = 2^p - 1$) of quantization intervals lying symmetrically around zero. Thus the approximation value 0.0 will be used for all wavelet coefficients lying close to zero.
The approximation error can be further reduced by adapting the partitioning of the coefficient interval to the frequency distribution of the wavelet coefficients. This technique is called a nonuniform scalar quantization or pdf-quantization. A finer partitioning resulting in a smaller approximation error is used in regions with many wavelet coefficients while a coarser partitioning increases the approximation error for regions with only few wavelet coefficients.
Usually the density function of a normal distribution is used as a model for the

[1] except those from the smooth residuum of the last transform step

frequency distribution of the wavelet coefficients:

$$f(x) \;=\; \frac{1}{\sigma\sqrt{2\pi}}\,\mathrm{e}^{-\frac{1}{2}\left(\frac{x-\mu}{\sigma}\right)^2}\,. \tag{20}$$

Since $\mu = 0$, the standard deviation σ of the coefficients is the only parameter to be fitted.

LLOYD and MAX [Llo57, Max60] have introduced an algorithm to adapt the partitioning of the coefficient interval to the model (20). Again, the (nonuniform) quantization intervals are numbered from $0, \ldots, n-1$ and these numbers are output as symbols to the coder. Note that for the dequantization step the standard deviation σ has to be stored in addition to the boundary values of the coefficient interval and the number n of subintervals.

3.2 Vector Quantization

Unlike the scalar case, a vector quantizer groups several wavelet coefficients together and outputs a single symbol for this coefficient vector. On the one hand, this can greatly reduce the number of different symbols needed, on the other hand, the approximation error might become too large. It is the crucial point of every vector quantizer to use a carefully chosen set of *code vectors*, which act as representatives for the coefficient vectors. For every coefficient vector, its best matching code vector is determined, and the number of this code vector is output to the coder. In the dequantization step, a code vector is used as an approximation for all the coefficient vectors which have been mapped to this code vector. The best matching code vector for a particular coefficient vector is the one which minimizes the Euclidian distance to the coefficient vector among all code vectors.

The most important aspect of vector quantization is the computation of the *codebook*, i.e. the set of all code vectors. This task has been studied by LINDE, BUZO and GRAY [LBG80]. They proposed an iterative algorithm called the *LBG algorithm*, which converges against a local optimal codebook. An even better adapted codebook can be obtained by using our modified LBG algorithm, see [HS00].

4 Coding

The final step in the compression scheme takes the symbols from the quantizer and codes them into a bitstream, which can be written to a file. The coding itself is losslessly invertible. Many different coding schemes have been developed and studied, ranging from a fast but usually not very efficient run-length coding over a variable code size Huffman coding [Huf52] to any of the variants of a quite efficient but computationally expensive arithmetic coding [Pas76, RL79,

WNC87]). Instead of re-describing these well-known coding techniques, we refer to the literature mentioned before or to the excellent textbook by GERSHO and GRAY [GG92], which covers these aspects as well.
One aspect of coding deserves special attention: more efficient coding schemes like Huffman coding or arithmetic coding use a variable code size for each input symbol depending on the symbol's probability of occurence. However, the latter is unknown to the coder a priori. Therefore the coder has to adapt to the probabilities of occurence with every new symbol being coded. Again we refer to [GG92] for a detailed description of this adaptive control.

5 Implementation

Our framework for evaluating the quality of lossy image compression consists of several independent modules, which can be easily exchanged or extended. The following list gives a brief overview of the capabilities of our system:

- wavelet transform:
  - many different pre-defined wavelets + user-definable wavelets
  - MALLAT algorithm
  - best-basis algorithm
- quantization:
  - uniform scalar quantization
  - non-uniform scalar quantization
  - vector quantization
- coding:
  - adaptive arithmetic coding
  - adaptive arithmetic coding with preceeding run-length coding

The coefficients of the wavelets available in our framework are taken from [Dau92, SS96, BCR91, Dau93, ASH87, ABDM92, VBL95, VTC96, OB96, Bri93]. Additional wavelets can be integrated easily by the user. Both wavelet transforms are implemented as described in Section 2.3.
For the quantization step we implemented the techniques from Section 3.1 and 3.2. In order to find an optimal bit allocation for the quantization of the subbands [JN84, GS88], we use a numerical bisection method to minimize a cost functional subject to auxiliary conditions (LAGRANGE method).

Our coding scheme is restricted to an adaptive arithmetic coder [BCW90], which has been modified to be optionally preceeded by a run-length coding step. The arithmetic coding is performed in integer arithmetics, the adaption of the coding to the input data follows the technique presented in [GG92, Sec. 9.7].

6 Results

One major aspect that influenced the development of our framework was to compare different parameter settings for each of the compression steps and to study their interdependecies. We chose several digitized images from both the *Hubble Space Telescope Archive* [HST99] and the FBI fingerprint archive [Bri96]. These two archives are denoted as *scenarios* in the following. Some of the chosen test images are shown in Figure 4 and Figure 5. For each of the test images we performed numerous compression–decompression–comparison cycles using different parameter settings each time. The following parameters have been varied according to the given ranges:

1. choice of the wavelet: 18 different wavelets have been examined; the most useful wavelets for image compression according to our tests are printed in Table 1 (page 15);
2. choice of the transform algorithm (MALLAT vs. best-basis);
3. number of levels of resolution ($M = 3, \ldots, 8$);
4. choice of quantization technique: uniform scalar, non-uniform scalar, and vector quantization; using vector quantization, the codebook size $n = 2^p$, $p = 7, \ldots, 10$ and the code vector length $l = 4, 16$ have been varied as well (see [HS00] for details);
5. choice of coding scheme: adaptive arithmetic coder with or without preceeded run-length coding.

All combinations of settings for these parameters have been evaluated and analyzed. The decompressed images have been compared to the original images using both the well-know ***p**eak-**s**ignal-to-**n**oise **r**atio* (PSNR) and the ***d**istortion **m**easure adapted to **h**uman **p**erception* (DMHP) proposed in [BWW96]. A detailed description of the results has been published in [Hab99]. In this report we wil give a short summary of the results obtained. It is worthwhile to note that these results differ only very little between different images within each scenario. Therefore we present the results grouped by the two scenarios investigated.

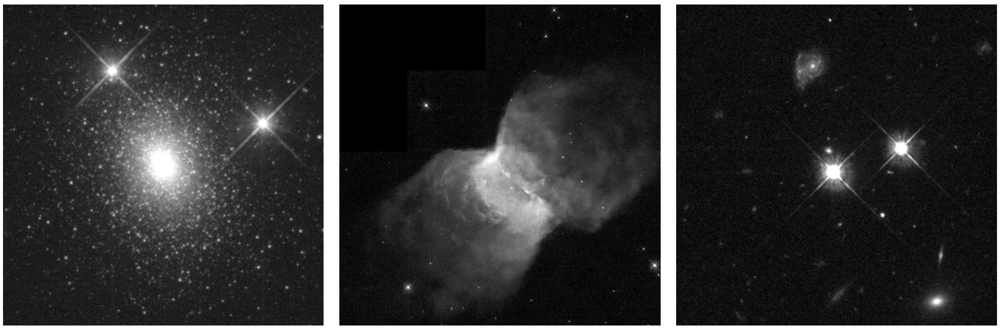

Figure 4: Images from the *Hubble Space Telescope Archive* [HST99]

Figure 5: Images from the fingerprint archive of the FBI [Bri96]

6.1 Astronomy Scenario

The results of our simulations using images from the astronomy scenario can be summarized as follows:

- very good results are obtained by using the wavelets $\mathcal{W}_1$, $\mathcal{W}_2$ and the MALLAT algorithm with $M = 5, \ldots, 8$ levels of resolution;
- using the best-basis algorithm with $M = 5, \ldots, 7$, the wavelet $\mathcal{W}_1$ produces very good results as well;
- uniform scalar quantization produces better results than non-uniform scalar quantization (see remark in Section 6.3);
- vector quantization yields outstanding results compared to scalar quantization: a code vector length of $l = 16$ should be chosen always, a codebook size of $n \geq 256$ is usually sufficient to produce better results than a scalar quantization (cf. Section 6.3);

- an additional run-length coding step before the arithmetic coding leads to very little improvement of the results.

6.2 Fingerprint Scenario

For the fingerprint scenario, the following observations have been made:

- the wavelet $\mathcal{W}_3$ yields very good results using the MALLAT algorithm and $M = 4, \ldots, 7$ levels of resolution;
- even better results are produced by using the wavelets $\mathcal{W}_1$, $\mathcal{W}_3$ and the best-basis algorithm with $M = 4, \ldots, 6$;
- concerning the quantization step, the same observations as stated in Section 6.1 have been made; the only difference is that a code vector length of $l = 4$ yields better results for small codebook sizes $n \leq 256$ in this scenario;
- the benefit of an additional run-length coding step before the arithmetic coding depends heavily on the quantization technique being used: it is recommended to use a run-length coding in combination with a uniform quantization; there is no improvement when using vector quantization.

6.3 Summary

Our simulations showed that it is possible to find a common set of parameters for each of the examined scenarios, which leads to very good results in the average when compressing arbitrary images from theses scenarios. We suggest to run a similar parameter analysis in all cases, where a huge number of images from a single scenario has to be compressed.

However, some observations from our simulations need to be explained in more detail. At first glance, one expects from a non-uniform scalar quantizer to produce better results than a uniform scalar quantizer. Our results showed correctly, that this is generally not the case. The reason for this unexpected behaviour is given by the entropy coding step that follows the quantization step. A non-uniform quantizer generates symbols whose probabilities of occurence are rather uniformly distributed. This is actually the worst case for any entropy coding! To our knowledge, the only published statement about this fact is given in [GG92, Sec. 9.9]: "... *a uniform quantizer is approximately optimal if entropy coding is used.*"

Vector quantization has proven to be a very powerful technique in our simulations. Even though the computational costs for compressing images can become quite high, the advantage of fast decompression and high reconstruction quality (given a fixed compression ratio) cannot be neglected. Our simulations show, that one codebook is sufficient for all images from one scenario. Such a scenario-based codebook can be computed once and does not have to be stored with the compressed data. In this case, a codebook size of $n = 1024$ produces very good results.

7 Conclusions and Future Work

In this research report we describe a framework for determining the quality of lossy image compression techniques based on a wavelet decomposition of the image data. Our framework offers several possibilities to perform each of the three steps "transform — quantization — coding" characteristic for this compression technique.

From our simulations we can conclude that it is indeed worth the effort to perform an analysis on several images of a scenario and find a (scenario dependend) set of compression parameters, if a large number of images from a single scenario has to be compressed subject to a high reconstruction quality.

It is left as a future work task to develop techniques and algorithms that are able to find a (sub-)optimal set of compression parameters without evaluating all possible parameter combinations. Such techniques might use available image information like for instance color / gray tone histograms or frequency distributions obtained through a Fast Fourier Transform to restrict the space of parameter combinations being evaluated.

Table 1: Wavelet coefficients (orthogonal wavelets have identical coefficients for analysis (A) and synthesis (S), biorthogonal wavelets have different coefficients for each)

name	mask coefficients	reference
$\mathcal{W}_1$	A + S: $\{ -3.793512864380802 \cdot 10^{-3}$, $7.782596425672746 \cdot 10^{-3}$, $2.345269614207717 \cdot 10^{-2}$, $-6.577191128146936 \cdot 10^{-2}$, $-6.112339000297255 \cdot 10^{-2}$, $4.051769024091182 \cdot 10^{-1}$, $7.937772226260872 \cdot 10^{-1}$, $4.284834763773700 \cdot 10^{-1}$, $-7.179982161915484 \cdot 10^{-2}$, $-8.230192710629983 \cdot 10^{-2}$, $3.455502757329774 \cdot 10^{-2}$, $1.588054486366945 \cdot 10^{-2}$, $-9.007976136730624 \cdot 10^{-3}$, $-2.574517688136797 \cdot 10^{-3}$, $1.117518770830630 \cdot 10^{-3}$, $4.662169598204029 \cdot 10^{-4}$, $-7.098330250637900 \cdot 10^{-5}$, $-3.459977319727278 \cdot 10^{-5} \}$	[BCR91, Dau93]
$\mathcal{W}_2$	A: $\{ 3.782845550699546 \cdot 10^{-2}$, $-2.384946501938000 \cdot 10^{-2}$, $-1.106244044184234 \cdot 10^{-1}$, $3.774028556126538 \cdot 10^{-1}$, $8.526986790094034 \cdot 10^{-1}$, $3.774028556126538 \cdot 10^{-1}$, $-1.106244044184234 \cdot 10^{-1}$, $-2.384946501938000 \cdot 10^{-2}$, $3.782845550699546 \cdot 10^{-2} \}$ S: $\{ -6.453888262893844 \cdot 10^{-2}$, $-4.068941760955844 \cdot 10^{-2}$, $4.180922732222122 \cdot 10^{-1}$, $7.884856164056644 \cdot 10^{-1}$, $4.180922732222122 \cdot 10^{-1}$, $-4.068941760955844 \cdot 10^{-2}$, $-6.453888262893844 \cdot 10^{-2} \}$	[ABDM92], [VBL95]

continued on next page

name	mask coefficients	reference
$\mathcal{W}_3$	A: $\{ 2.885256501123136 \cdot 10^{-2},$ $8.244478227504624 \cdot 10^{-5},$ $-1.575264469076351 \cdot 10^{-1},$ $7.679048884691436 \cdot 10^{-2},$ $7.589077294537619 \cdot 10^{-1},$ $7.589077294537619 \cdot 10^{-1},$ $7.679048884691436 \cdot 10^{-2},$ $-1.575264469076351 \cdot 10^{-1},$ $8.244478227504624 \cdot 10^{-5},$ $2.885256501123136 \cdot 10^{-2} \}$ S: $\{ 9.544158682436510 \cdot 10^{-4},$ $-2.727196296995984 \cdot 10^{-6},$ $-9.452462998353147 \cdot 10^{-3},$ $-2.528037293949898 \cdot 10^{-3},$ $3.083373438534267 \cdot 10^{-2},$ $-1.376513483818652 \cdot 10^{-2},$ $-8.566118833165885 \cdot 10^{-2},$ $1.633685405569888 \cdot 10^{-1},$ $6.233596410344158 \cdot 10^{-1},$ $6.233596410344158 \cdot 10^{-1},$ $1.633685405569888 \cdot 10^{-1},$ $-8.566118833165885 \cdot 10^{-2},$ $-1.376513483818652 \cdot 10^{-2},$ $3.083373438534267 \cdot 10^{-2},$ $-2.528037293949898 \cdot 10^{-3},$ $-9.452462998353147 \cdot 10^{-3},$ $-2.727196296995984 \cdot 10^{-6},$ $9.544158682436510 \cdot 10^{-4} \}$	[VTC96]

References

[ABDM92] Marc Antonini, Michel Barlaud, Ingrid Daubechies, and Pierre Mathieu. Image Coding using Wavelet Transform. *IEEE Transactions on Image Processing*, 1(2):205–220, April 1992.

[ABM91] Marc Antonini, Michel Barlaud, and Pierre Mathieu. Digital Image Compression using Vector Quantisation and the Wavelet Transform. In Yves Meyer, editor, *Wavelets and Applications*, number 20 in Research Notes in Applied Mathematics, pages 160–174. Springer–Verlag, 1991.

[ASH87] Edward H. Adelson, Eero P. Simoncelli, and Rajesh Hingorani. Orthogonal Pyramid Transforms for Image Coding. In *Visual Communications and Image Processing II*, volume 845 of *SPIE*, pages 50–58, Cambridge, MA, October 1987.

[BA83] Peter J. Burt and Edward H. Adelson. The Laplacian Pyramid as a Compact Image Code. *IEEE Transactions on Communications*, 31(4):532–540, April 1983.

[Bal98] Ilangko Balasingham. *On Optimal Perfect Reconstruction Filter Banks for Image Compression*. PhD thesis, Department of Telecommunications, Norwegian University of Science and Technology, Trondheim, Norway, 1998.

[BCR91] Gregory Beylkin, Ronald R. Coifman, and Vladimir Rokhlin. Fast Wavelet Transforms and Numerical Algorithms I. *Communications on Pure and Applied Mathematics*, 44:141–183, 1991.

[BCW90] Timothy C. Bell, John G. Cleary, and Ian H. Witten. *Text Compression*. Prentice–Hall International, New Jersey, 1990.

[Bri93] Christopher M. Brislawn. Classification of Symmetric Wavelet Transforms. Technical Report LA-UR-92-2823, Los Alamos National Laboratory, Los Alamos, NM, March 1993.

[Bri96] Christopher M. Brislawn. The FBI Fingerprint Image Compression Standard. WWW: `http://www.c3.lanl.gov/~brislawn/FBI/FBI.html`, July 1996.

[BWW96] Franziska Bock, Horst Walter, and Matthias Wilde. A New Distortion Measure for the Assessment of Decoded Images Adapted to Human Perception. In *Proceedings of the 3rd International Workshop in Image/Signal Processing*, Manchester, November 1996.

[Chu92] Charles K. Chui. *An Introduction to Wavelets*, volume 1 of *Wavelet Analysis and its Application*. Academic Press, London, 1992.

[CS94] Christos Chrysafis and Michael G. Strintzis. Design of Filters for Minimum Variance Multiresolution Analysis and Subband Decomposition. In *SPIE Conference on Visual Communications and Image Processing*, Chicago, IL, September 1994.

[CW90] Ronald R. Coifman and Mladen V. Wickerhauser. Best-Adapted Wave Packet Bases. Preprint, Yale University, New Haven, February 1990.

[CW92] Ronald R. Coifman and Mladen V. Wickerhauser. Entropy-Based Algorithms for Best Basis Selection. *IEEE Transactions on Information Theory*, 38(2):713–718, March 1992.

[Dau92] Ingrid Daubechies. *Ten Lectures on Wavelets*, volume 61 of *CBMS-NSF Regional Conference Series in Applied Mathematics*. Society for Industrial and Applied Mathematics, Philadelphia, 1992.

[Dau93] Ingrid Daubechies. Orthonormal Bases of Compactly Supported Wavelets II. Variations on a Theme. *SIAM Journal on Mathematical Analysis*, 24(2):499–519, March 1993.

[Equ89] William H. Equitz. A New Vector Quantization Clustering Algorithm. *IEEE Transactions on Acoustics, Speech and Signal Processing*, 37(10):1568–1575, October 1989.

[GG92] Allen Gersho and Robert M. Gray. *Vector Quantization and Signal Compression*. Kluwer Academic Publishers, Massachusetts, 1992.

[GS88] Allen Gersho and Yair Shoham. Efficient Bit Allocation for an Arbitrary Set of Quantizers. *IEEE Transactions on Acoustics, Speech and Signal Processing*, 36(9):1445–1453, September 1988.

[Hab99] Jörg Haber. *Konstruktion und Implementierung eines neuen Verfahrens zur Kompression von Bilddaten*. PhD thesis, Technische Universität München, München, Germany, 1999.

[HS00] Jörg Haber and Hans-Peter Seidel. Using an Enhanced LBG-Algorithm to Reduce the Codebook Error in Vector Quantization. In *Proceedings of Computer Graphics International 2000 (CGI 2000)*. Springer–Verlag, 2000. accepted for publication.

[HST99] General Overview of the Hubble Space Telescope. WWW: `http://www.stsci.edu/hst`, February 1999.

[HSW95] Peter N. Heller, Jerome M. Shapiro, and Raymond O. Wells, Jr. Optimally smooth symmetric quadrature mirror filters for image coding. In *Wavelet Applications II (Proc. of the SPIE)*, volume 2491, pages 119–130, Orlando, FL, April 1995.

[Huf52] David A. Huffman. A Method for the Construction of Minimum-Redundancy Codes. *Proceedings of the IRE*, 40(9):1098–1101, September 1952.

[Jac92] Arnaud Jacquin. Image Coding Based on a Fractal Theory of Iterated Contractive Image Transformations. *IEEE Transactions on Image Processing*, 1(1):18–30, January 1992.

[JN84] Nuggehally S. Jayant and Peter Noll. *Digital Coding of Waveforms*. Prentice–Hall International, New Jersey, 1984.

[Kar47] Kari Karhunen. Über Lineare Methoden in der Wahrscheinlichkeitsrechnung. *Annales Academiae Scientiarum Fennicae*, 37:3–79, 1947.

[LBG80] Yoseph Linde, Andres Buzo, and Robert M. Gray. An Algorithm for Vector Quantizer Design. *IEEE Transactions on Communications*, 28(1):84–95, January 1980.

[Llo57] Stuart P. Lloyd. Least Squares Quantization in PCM. Technical report, Bell Telephone Laboratories, Murray Hill, NJ, 1957.

[Llo82] Stuart P. Lloyd. Least Squares Quantization in PCM. *IEEE Transactions on Information Theory*, 28:129–137, March 1982.

[Loè48] Michel Loève. Fonctions Aleatoires de Seconde Ordre. In P. Lévy, editor, *Processus Stochastiques et Mouvement Brownien*. Gauthier Villars, Paris, 1948.

[Mal89] Stephane G. Mallat. A Theory for Multiresolution Signal Decomposition: The Wavelet Representation. *IEEE Transactions on Pattern Analysis and Machine Intelligence*, 11(7):674–693, July 1989.

[Max60] J. Max. Quantizing for Minimum Distortion. *IEEE Transactions on Information Theory*, 6(1):7–12, March 1960.

[Mey92] Yves Meyer. *Wavelets and Operators*. Cambridge University Press, Cambridge, MA, 1992.

[OB96] Jan E. Odegard and C. Sidney Burrus. Smooth Biorthogonal Wavelets for Applications in Image Compression. In *Proceedings of the* 7^{th} *DSP Workshop*, pages 73–76, Loen, Norwegen, September 1996.

[Pas76] Richard C. Pasco. *Source Coding Algorithms for Fast Data Compression*. PhD thesis, Stanford University, Palo Alto, CA, 1976.

[PM93] William B. Pennebaker and Joan L. Mitchell. *JPEG — Still Image Data Compression Standard*. Van Nostrand Reinhold, New York, 1993.

[RL79] Jorma J. Rissanen and Glen G. Langdon. Arithmetic Coding. *IBM Journal of Research and Development*, 23(2):149–162, March 1979.

[Sau95] Dietmar Saupe. Fractal Image Compression via Nearest Neighbor Search. In Yuval Fisher, editor, *Proc. NATO ASI Fractal Image Encoding and Analysis, Trondheim*, July 1995. to appear in Springer–Verlag, New York, 1997.

[Say96] Khalid Sayood. *Introduction to Data Compression*. Morgan Kaufman Publishers, Inc., San Francisco, CA, 1996.

[Sha93] Jerome M. Shapiro. Embedded Image Coding using Zerotrees of Wavelet Coefficients. *IEEE Transactions on Signal Processing*, 41(12):3445–3462, December 1993.

[SN96] Gilbert Strang and Truong Nguyen. *Wavelets and Filter Banks*. Wellesley-Cambridge Press, Wellesley, MA, 1996.

[SS96] Jianhong Shen and Gilbert Strang. Asymptotic Analysis of Daubechies Polynomials. *Proceedings of the AMS*, 124(12):3819–3833, December 1996.

[VBL95] John D. Villasenor, Benjamin Belzer, and Judy Liao. Wavelet Filter Evaluation for Image Compression. *IEEE Transactions on Image Processing*, 4(8):1053–1060, August 1995.

[VK95] Martin Vetterli and Jelena Kovačević. *Wavelets and Subband Coding*. Prentice–Hall International, New Jersey, 1995.

[VTC96] John D. Villasenor, Min-Jen Tsai, and Feng Chen. Stack-run Image Coding. *IEEE Transactions on Circuits and Systems for Video Technology*, 6:519–521, October 1996.

[Wic90] Mladen V. Wickerhauser. Picture Compression by Best-Basis SubBand Coding. Preprint, Yale University, New Haven, 1990.

[WNC87] Ian H. Witten, Radford M. Neal, and John G. Cleary. Arithmetic Coding for Data Compression. *Communications of the ACM*, 30(6):520–540, June 1987.

I N F O R M A T I K

Below you find a list of the most recent technical reports of the Max-Planck-Institut für Informatik. They are available by anonymous ftp from `ftp.mpi-sb.mpg.de` under the directory `pub/papers/reports`. Most of the reports are also accessible via WWW using the URL `http://www.mpi-sb.mpg.de`. If you have any questions concerning ftp or WWW access, please contact `reports@mpi-sb.mpg.de`. Paper copies (which are not necessarily free of charge) can be ordered either by regular mail or by e-mail at the address below.

Max-Planck-Institut für Informatik

Library

attn. Anja Becker

Im Stadtwald

66123 Saarbrücken

GERMANY

e-mail: `library@mpi-sb.mpg.de`

MPI-I-1999-3-005	T.A. Henzinger, J. Raskin, P. Schobbens	Axioms for Real-Time Logics
MPI-I-1999-3-004	J. Raskin, P. Schobbens	Proving a conjecture of Andreka on temporal logic
MPI-I-1999-3-003	T.A. Henzinger, J. Raskin, P. Schobbens	Fully Decidable Logics, Automata and Classical Theories for Defining Regular Real-Time Languages
MPI-I-1999-3-002	J. Raskin, P. Schobbens	The Logic of Event Clocks
MPI-I-1999-3-001	S. Vorobyov	New Lower Bounds for the Expressiveness and the Higher-Order Matching Problem in the Simply Typed Lambda Calculus
MPI-I-1999-2-008	A. Bockmayr, F. Eisenbrand	Cutting Planes and the Elementary Closure in Fixed Dimension
MPI-I-1999-2-007	G. Delzanno, J. Raskin	Symbolic Representation of Upward-closed Sets
MPI-I-1999-2-006	A. Nonnengart	A Deductive Model Checking Approach for Hybrid Systems
MPI-I-1999-2-005	J. Wu	Symmetries in Logic Programs
MPI-I-1999-2-004	V. Cortier, H. Ganzinger, F. Jacquemard, M. Veanes	Decidable fragments of simultaneous rigid reachability
MPI-I-1999-2-003	U. Waldmann	Cancellative Superposition Decides the Theory of Divisible Torsion-Free Abelian Groups
MPI-I-1999-2-001	W. Charatonik	Automata on DAG Representations of Finite Trees
MPI-I-1999-1-007	C. Burnikel, K. Mehlhorn, M. Seel	A simple way to recognize a correct Voronoi diagram of line segments
MPI-I-1999-1-006	M. Nissen	Integration of Graph Iterators into LEDA
MPI-I-1999-1-005	J.F. Sibeyn	Ultimate Parallel List Ranking ?
MPI-I-1999-1-004	M. Nissen, K. Weihe	How generic language extensions enable “open-world” desing in Java
MPI-I-1999-1-003	P. Sanders, S. Egner, J. Korst	Fast Concurrent Access to Parallel Disks
MPI-I-1999-1-002	N.P. Boghossian, O. Kohlbacher, H.-. Lenhof	BALL: Biochemical Algorithms Library
MPI-I-1999-1-001	A. Crauser, P. Ferragina	A Theoretical and Experimental Study on the Construction of Suffix Arrays in External Memory
MPI-I-98-2-018	F. Eisenbrand	A Note on the Membership Problem for the First Elementary Closure of a Polyhedron
MPI-I-98-2-017	M. Tzakova, P. Blackburn	Hybridizing Concept Languages
MPI-I-98-2-014	Y. Gurevich, M. Veanes	Partisan Corroboration, and Shifted Pairing
MPI-I-98-2-013	H. Ganzinger, F. Jacquemard, M. Veanes	Rigid Reachability

MPI-I-98-2-012	G. Delzanno, A. Podelski	Model Checking Infinite-state Systems in CLP
MPI-I-98-2-011	A. Degtyarev, A. Voronkov	Equality Reasoning in Sequent-Based Calculi
MPI-I-98-2-010	S. Ramangalahy	Strategies for Conformance Testing
MPI-I-98-2-009	S. Vorobyov	The Undecidability of the First-Order Theories of One Step Rewriting in Linear Canonical Systems
MPI-I-98-2-008	S. Vorobyov	AE-Equational theory of context unification is Co-RE-Hard
MPI-I-98-2-007	S. Vorobyov	The Most Nonelementary Theory (A Direct Lower Bound Proof)
MPI-I-98-2-006	P. Blackburn, M. Tzakova	Hybrid Languages and Temporal Logic
MPI-I-98-2-005	M. Veanes	The Relation Between Second-Order Unification and Simultaneous Rigid *E*-Unification
MPI-I-98-2-004	S. Vorobyov	Satisfiability of Functional+Record Subtype Constraints is NP-Hard
MPI-I-98-2-003	R.A. Schmidt	E-Unification for Subsystems of S4
MPI-I-98-2-002	F. Jacquemard, C. Meyer, C. Weidenbach	Unification in Extensions of Shallow Equational Theories
MPI-I-98-1-031	G.W. Klau, P. Mutzel	Optimal Compaction of Orthogonal Grid Drawings
MPI-I-98-1-030	H. Brönniman, L. Kettner, S. Schirra, R. Veltkamp	Applications of the Generic Programming Paradigm in the Design of CGAL
MPI-I-98-1-029	P. Mutzel, R. Weiskircher	Optimizing Over All Combinatorial Embeddings of a Planar Graph
MPI-I-98-1-028	A. Crauser, K. Mehlhorn, E. Althaus, K. Brengel, T. Buchheit, J. Keller, H. Krone, O. Lambert, R. Schulte, S. Thiel, M. Westphal, R. Wirth	On the performance of LEDA-SM
MPI-I-98-1-027	C. Burnikel	Delaunay Graphs by Divide and Conquer
MPI-I-98-1-026	K. Jansen, L. Porkolab	Improved Approximation Schemes for Scheduling Unrelated Parallel Machines
MPI-I-98-1-025	K. Jansen, L. Porkolab	Linear-time Approximation Schemes for Scheduling Malleable Parallel Tasks
MPI-I-98-1-024	S. Burkhardt, A. Crauser, P. Ferragina, H. Lenhof, E. Rivals, M. Vingron	q-gram Based Database Searching Using a Suffix Array (QUASAR)
MPI-I-98-1-023	C. Burnikel	Rational Points on Circles
MPI-I-98-1-022	C. Burnikel, J. Ziegler	Fast Recursive Division
MPI-I-98-1-021	S. Albers, G. Schmidt	Scheduling with Unexpected Machine Breakdowns
MPI-I-98-1-020	C. Rüb	On Wallace's Method for the Generation of Normal Variates
MPI-I-98-1-019		2nd Workshop on Algorithm Engineering WAE '98 - Proceedings
MPI-I-98-1-018	D. Dubhashi, D. Ranjan	On Positive Influence and Negative Dependence
MPI-I-98-1-017	A. Crauser, P. Ferragina, K. Mehlhorn, U. Meyer, E. Ramos	Randomized External-Memory Algorithms for Some Geometric Problems
MPI-I-98-1-016	P. Krysta, K. Loryś	New Approximation Algorithms for the Achromatic Number
MPI-I-98-1-015	M.R. Henzinger, S. Leonardi	Scheduling Multicasts on Unit-Capacity Trees and Meshes
MPI-I-98-1-014	U. Meyer, J.F. Sibeyn	Time-Independent Gossiping on Full-Port Tori
MPI-I-98-1-013	G.W. Klau, P. Mutzel	Quasi-Orthogonal Drawing of Planar Graphs
MPI-I-98-1-012	S. Mahajan, E.A. Ramos, K.V. Subrahmanyam	Solving some discrepancy problems in NC*